

# We are IntechOpen, the world's leading publisher of Open Access books Built by scientists, for scientists

6,900

Open access books available

185,000

International authors and editors

200M

Downloads

Our authors are among the

154

Countries delivered to

TOP 1%

most cited scientists

12.2%

Contributors from top 500 universities



WEB OF SCIENCE™

Selection of our books indexed in the Book Citation Index  
in Web of Science™ Core Collection (BKCI)

Interested in publishing with us?  
Contact [book.department@intechopen.com](mailto:book.department@intechopen.com)

Numbers displayed above are based on latest data collected.  
For more information visit [www.intechopen.com](http://www.intechopen.com)



# Development of a Low-Cost Vibration Damper Dynamometer for Suspension Damper Testing

*Yucheng Liu and Ge He*

## Abstract

On performance vehicles, suspension dampers are used to reduce the vibration produced by variations in the driving surface, while simultaneously controlling the rate of load transfer between tires during lateral and longitudinal acceleration. To measure the characteristics of suspension dampers, a damper dynamometer is typically used to compress and elongate the dampers at a known speed, and then measure the force output. However, a commercial damper dynamometer is usually expensive and not always suitable for the dampers specifically designed for a customized vehicle. In this chapter, a cheap, customized, and effective damper dynamometer is constructed through computer-aided design, finite element analysis, and manufacture to measure the properties of suspension dampers used in a racecar. It was demonstrated through data analysis that this designed damper dynamometer can produce usable measurement data for a far lower cost than other methods.

**Keywords:** suspension damper, damper dynamometer, computer-aided design, finite element analysis

## 1. Introduction

Dampers are being successfully and widely used to reduce vibrations in most applications, such as civil engineering structures and automotive components. In civil engineering [1–4], for example, adding fluid viscous dampers to buildings can help protect buildings, bridges, and other structures in a variety of scenarios including seismic events, strong winds, and pedestrian energy. For automotive engineering, proper suspension damping reduces the vibration produced by variations in the driving surface, while simultaneously controlling the rate of load transfer between tires during lateral and longitudinal acceleration. Because these damping modes occur at different speeds of compression and rebound (elongation), the best racing dampers offer damping rate adjustments at both high and low speeds.

For at least the past 4 years, our team has used Ohlins TTX25 MkII dampers on its racecars, seen in **Figure 1**. These dampers retail at \$650 each, but they include the high- and low-speed damping rate adjustments necessary for optimal damper performance. For an independent suspension vehicle, this comes to a total cost of \$2600, offering the team a significant financial incentive to reuse them between design cycles. Luckily, the manufacturer offers detailed documentation on how



**Figure 1.**  
*Öhlins TTX25 MkII dampers.*

to perform proper maintenance, so the team performs full damper rebuilds when reusing the dampers on a new car.

One drawback of rebuilding dampers is the inability to easily tell whether their performance will remain unchanged after the rebuild. This can lead to different damping rates on each corner of the car, resulting in less than ideal performance of the car's suspension. To prevent this, it is important to measure the characteristics of each damper after rebuilding it. However, unlike springs, the damping characteristics cannot be determined from simple static measurements and sophisticated devices,



**Figure 2.**  
*Intercomp 3HP shock dyno 1.0–55 in/s (\$8895.00).*

such as damper dynamometers are required to correctly measure them [5–7]. A damper dynamometer is a specialized machine that compresses and elongates the dampers at a known speed and then measures the force output. Market offerings for damper dynamometers are well outside the team's price range, with all viable options costing thousands of dollars, such as the Intercomp model shown in **Figure 2**.

These devices facilitate easy and straightforward measurement and data processing, but the trade-off in price is too high for the team to justify for such a specialty tool. An alternative option offered online is mailing the rebuilt dampers to a company specializing in damping rate measurement. Priced at around \$600 total, this route represents a significant decrease in cost, but still a relatively high yearly expense for the team. In addition, this would only enable the team to measure their dampers in a single setting, eliminating much of the team's ability to accurately compare the effects of different damping rates on the car. In light of the limitations and costs associated with the commercial damper measurement options available to the team, it was determined that the best course of action would be to design and manufacture a custom damper dynamometer catered to the specific needs of the team. Three primary requirements were established, in order of importance. While the custom damper dynamometer is temporarily used for characterizing the vehicle dampers, it is expected that the same design method can also be adopted for designing a custom dynamometer measuring damping rates of civil engineering structures. The design method described in this paper can also help increase the efficiency in designing dampers that are used for vibration control.

## 2. Design requirements

The most important requirement was that the dynamometer must produce usable measurement data. This was the primary purpose of the project and so takes priority over all other goals. The desired output of the dynamometer is a relationship between the compression/rebound rate and the resistive force output by the damper. Data should be measured at a rate of approximately 100 Hz for each sensor, comparable to the typical rate of data measurement the team uses when logging track data. The range of necessary compression and rebound speeds varies by damper; however, the FSAE team is primarily concerned with speeds up to 10 in/s. This corresponds with the maximum tested speed in the available force-velocity data for the Öhlins TTX25 MkII. The measurement device should maintain linearity up to at least 250 lbf of damper resistive force, which is the maximum force output achieved in the available force-velocity data for the dampers.

The second requirement was that the design would utilize wherever possible components that the team already owned. This was to reduce the cost of the project as much as possible, important for keeping it a viable financial alternative to purchasing a dynamometer or sending off the team's dampers for measurement.

The third requirement was that all parts of the project were able to be completed within a single semester. As a single-semester-directed individual study, it was imperative that the project was approached in such a way that it would be completed before the deadline. This requirement was changed out of necessity due to the COVID-19 pandemic and resultant changes to the accessibility of university purchasing and machining resources. Though the timeframe of completion shifted, there was still only around a semester of available time to work on this project. Due to this, the design was required to be simple enough that almost everything could be made in-house, reducing the lead time that would result from having to order components.

### 3. Design

The design of the dynamometer, as seen in **Figure 3**, was obtained following an existing system engineering design process [8–14] and a combined experimental-computational approach [11, 12]. A crank-slider mechanism imparts a forced displacement to one end of the damper, while the other end is mounted to a cantilevered bar. A welded frame constructed from low-carbon steel angle stock holds the crank-slider mechanism together. In **Figure 3a**, some sections of the frame have been made transparent for ease of viewing other components, and the model does not include fastening hardware. **Figure 3b** shows the fabricated and setup dynamometer. Parallel alongside the damper is a linear potentiometer used on the team's racecars for the exact purpose of measuring damper displacement. Attached at the base of the cantilevered bar are two strain gauges to measure the strain in the bar, and indirectly, the resistive force of the damper. This is similar to the design of the Intercomp dynamometer, with several key changes to reduce the price.

For the crank mechanism, a section of a retired crankshaft from one of the team's old engines was utilized. The CBR600 engine it came from has a cylinder stroke of 42.5 mm, approximately 75% of the usable stroke of the damper, providing the necessary leeway for setup adjustment. This crankshaft was modified to fit inside one of the milling machine's R8 collets. A steel rod was tapered and threaded to match an existing threaded hole in the crankshaft, in order to ensure collinearity during welding. Also utilized was the connecting rod, along with its big end bearing inserts and a section of the wrist pin. Since these parts already have tight tolerances on their interfacing surfaces, they offered a perfect opportunity to eliminate free play in the system while also cutting the cost and machining time.

The slider portion of the crank-slider mechanism consists of a smooth-surfaced rod with clevises on each end, constrained to a single degree of freedom with a custom aluminum bushing block. Careful surface preparation and lubrication allowed for the use of a bushing rather than a more expensive linear ball bearing while preventing mechanism binding, which would result in extra stresses in the frame and torque applied to the mill.

The welded frame was subjected to finite element analysis in SolidWorks to determine its adequacy for the maximum expected forces. The forces applied in the finite element model included the 250 lbf maximum damper output force, reacted by the bolt holes of the bearing which supports the crank. Conservatively, it was assumed that the entirety of the force was reacted by the frame, when in actuality, the mill will resist a portion of the force. In addition, the transverse component of the force in the connecting rod was calculated at its most extreme angle. This force (58 lbf), and its associated moment about the Z-axis (143 lbf-in), was applied to the

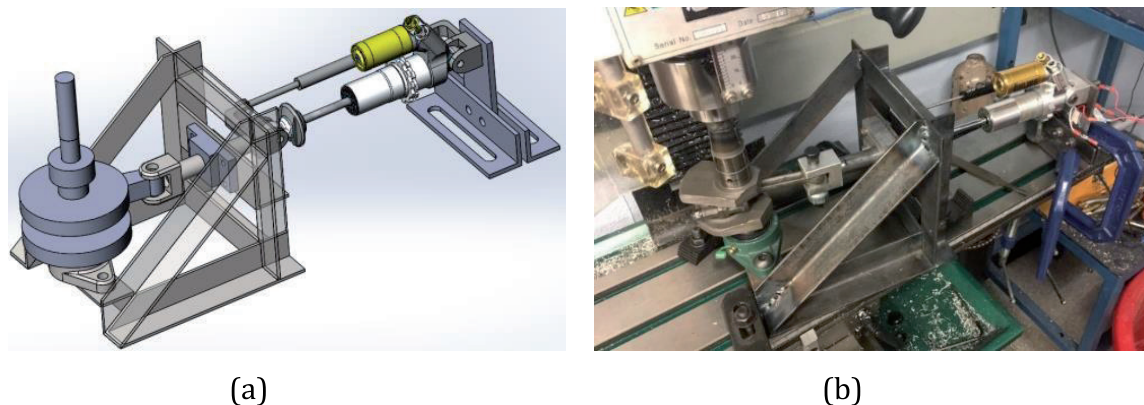


**Figure 3.**  
 (a) Damper dynamometer CAD model, (b) completed dynamometer setup.

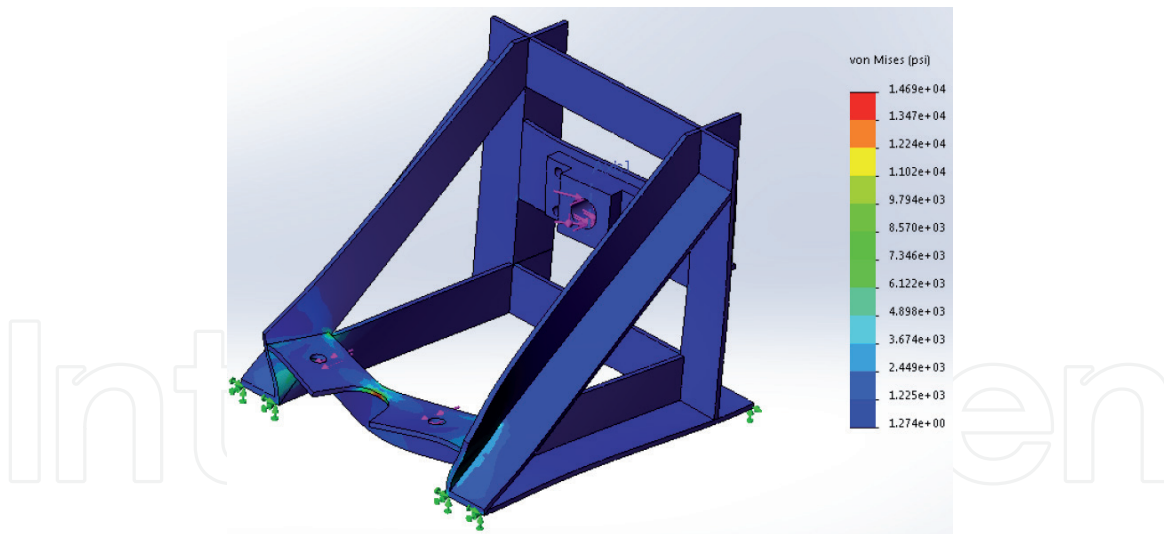


**Figure 4.**  
*Finite element simulation of dynamometer frame.*

aluminum bushing block that houses the slide rod. The finite element simulation result for this combined load case is shown in **Figure 4**.

As shown in **Figure 4**, the maximum stress experienced by the frame is 14.7 ksi. This corresponds to a factor of safety of approximately 3.7. At this point, further iteration could have reduced the weight of the frame. However, since weight was not a primary concern, it was decided that maintaining the thicker frame angles would result in easier welding operations. This will also allow the frame to potentially be used for testing larger dampers without modification.

The size of the cantilevered strain bar was chosen based on the expected output force of the dynamometer. For a set of available materials, the material thickness and width, as well as the magnitude and location of the applied force from the damper, were used to calculate the bending stress at the point where the strain bar was supported by its base. The chosen bar's thickness and width allow for a bending stress that is just below the yield stress for the material. At an applied force of 250 lbf and the designed cantilever moment arm of 2.375", a bending moment of 625 lbf-in is generated. The selected bar is composed of 1018 steel (yield strength = 53.7 ksi), with a rectangular cross-section of 2" width by 3/16" thickness. At the supported point where the bending stress is highest, this corresponds to an applied bending stress of approximately 50.7 ksi, or approximately 94% of the material's yield strength. This allows the bar to fully react the maximum expected force without yielding while maximizing the detectable elastic strain in the beam at lower force outputs. For higher damper force output applications in the future, a different cantilevered bar may be needed.

Used to measure the strain in the bar from the resistive force in the damper are two foil resistance strain gauges, nominally 350 ohm. Near the supported end of the strain bar, as close as possible to the point of maximum strain, the surface was prepared using progressively finer sandpaper. Strain gauges were attached to either face of the strain bar using a cyanoacrylate adhesive. The strain gauges (STRG1 and STRG2) were wired in a Wheatstone half-bridge configuration, according to the circuit diagram shown in **Figure 5**.

Originally, the bridge was completed using 350 ohm resistors, but these were swapped for 47 kohm resistors to limit the excessive noise seen in that half of the bridge, and to allow for the use of an available rotary potentiometer (POT 1) to effectively balance the bridge. The result is a steadier measurement of bridge imbalance, and the ability to center the measurement circuit output within the

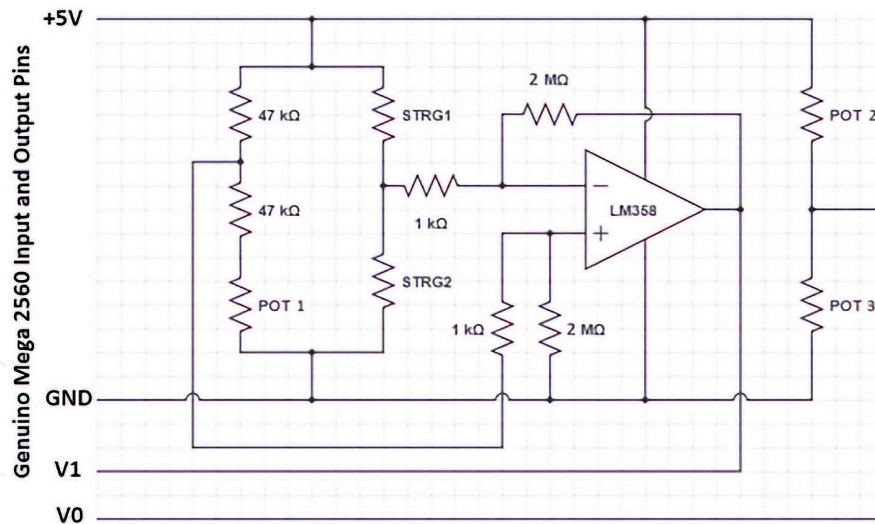


**Figure 5.**  
*Diagram of measurement circuit.*

measurable range of a Genuino Mega 2560 used for data capture. Using the Genuino as a 5 V supply voltage, the bridge imbalance is adjusted via the rotary potentiometer to account for imperfections in the manufacture and connection of the strain gauges. The voltage difference created by the bridge circuit under load is amplified using an LM358 op-amp chip in a differential amplifier configuration, also shown in **Figure 5**. The gain of the amplifier circuit is set at 2000 using a combination of 2 Mohm and 1 kohm resistors, so that the output is within the readable range of the Genuino and provides a large enough measurable range.

The linear potentiometer that measures the instantaneous length of the damper is represented on the far-right side of **Figure 5** as two variable resistors (POT 2 and POT 3), one of which increases resistance with increasing length and one of which decreases. The potentiometer uses a 5 V supply from the Genuino to output a maximum signal at full extension and a minimum signal at full compression.

Two input pins on the Genuino board (V0 and V1) are used to measure the op-amp output and the linear potentiometer output. The program loaded onto the board runs in a loop, conveying with each iteration the timestamp in milliseconds as well as a value between 0 and 1023 for each input pin. These values correspond to the voltage at each input pin, with the 0–5 V measurement range broken up evenly into 1024 subdivisions. A delay written into the program is adjusted to provide data points at a rate of 100 Hz, satisfying the data capture requirement outlined earlier.

These values are transmitted as comma-delimited serial data to the user's computer via USB, and the program RealTerm Serial/TCP Terminal is used to capture the data. After identifying the correct computer port for the incoming data transmission, RealTerm allows the dynamometer user to write all captured data to a text file, which is then parsed into Microsoft Excel for further analysis.

#### 4. Data analysis

The data is parsed into Microsoft Excel as a 4-column dataset. The data includes iteration number since the Genuino program began executing, timestamp in milliseconds since the program began executing, instantaneous voltage reading at input pin V0, and instantaneous voltage reading at pin V1. It should be noted that the raw data does not contain the initialization of the Genuino program, and thus the data does not begin at an iteration and timestamp of zero. This is acceptable because the

iteration number is only included to ensure that no steps have been skipped and the program is running properly.

The first step in analyzing the data is to establish a baseline for the strain gauge circuit output. Before turning on the milling machine to drive the dynamometer, several seconds of data are captured to establish an accurate baseline. In addition, the machine is turned off and allowed to rest for several more seconds before the capture program is terminated, in order to determine if the baseline changed during operation. This is possible if some components of the circuitry shift during the use of the dynamometer and warrant further attention and possibly recapture of the dataset.

The circuit used to measure the applied damper force was calibrated by mounting the cantilevered strain bar onto a vertical surface and applying known loads up to 200 lbs. at the location of the damper attachment, in intervals of 50 lbs. The linear potentiometer was calibrated by measuring the voltage output and comparing it to a measurement of displacement, in intervals of approximately 0.25 in. The results of these calibrations are shown in **Figures 6** and **7**.

Fitting a trend line to the calibration data shows that a high degree of linearity is maintained over the measured range. Because of the difficulty associated with accurately applying large known loads during calibration, it is necessary to assume that the linearity will hold true up to a load of 250 lbf. The high degree of linearity

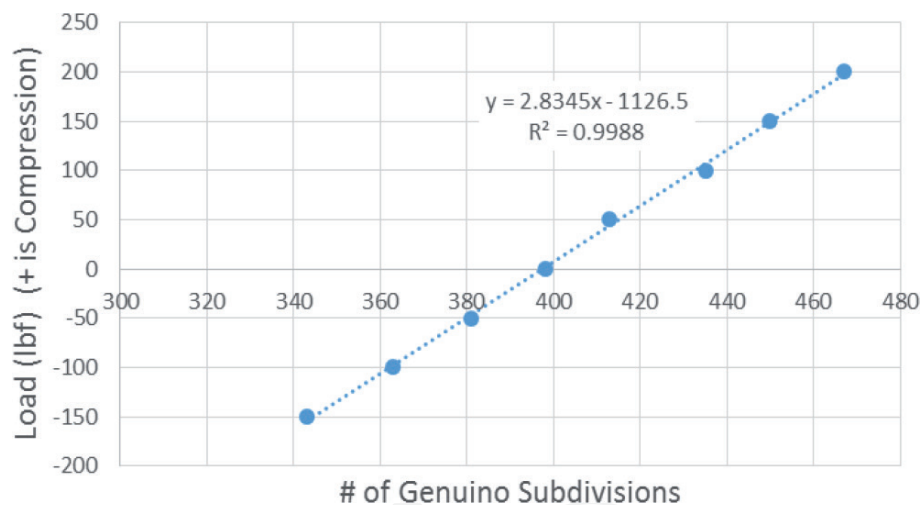


**Figure 6.**  
*Strain gauge calibration plot.*

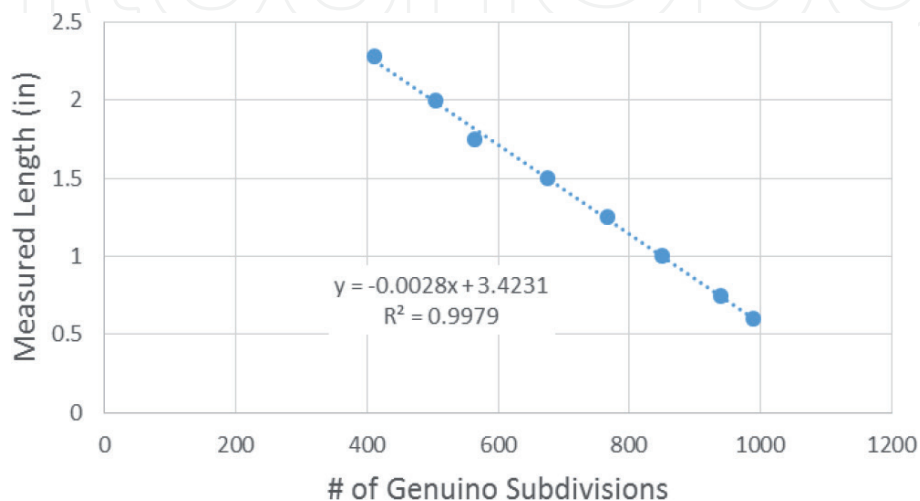


**Figure 7.**  
*Linear potentiometer calibration plot.*

seen in the calibration data justifies this assumption. From this data, the user can interpolate or extrapolate the applied load or displacement for a given Genuino voltage measurement.

After the sensors have been calibrated, it is possible to accurately plot the displacement of the driven end of the damper as a function of time. It is assumed that the strain bar contributes a negligible amount of displacement to the nondriven end of the damper. However, because the distance between the damper connection points is measured directly by the linear potentiometer, even without this assumption the measurement should be accurate. By taking the derivative of the displacement with respect to time, the compression or rebound velocity of the damper is obtained for each timestamp.

Because of noise in the measurement circuit, larger datasets are required to produce a smooth force-velocity curve for the damper. To analyze these large quantities of data, the method that was chosen is to take the average force-displacement over a range of input velocities. For example, the force and velocity data at all points which indicate a compression velocity of between  $-0.25$  in/s and  $0.25$  in/s is averaged to produce a single data point. The same is done for all points which indicate a compression velocity of between  $0.25$  in/s and  $0.75$  in/s, and so on, until the entire data set is accounted for. The same process is performed for rebound velocities.

Force-velocity graphs were generated for the range of adjustments listed in the available data from the manufacturer. The graphs sweep through a range of low-speed settings at the maximum high-speed setting, and a range of high-speed settings at the maximum low-speed setting. The naming convention of the graphs is chosen as LS-HS, where LS is low speed and HS is high speed. Low-speed settings are counted in clicks from fully closed, whereas high-speed settings are counted in revolutions from fully open. Thus, a graph labeled 0-3 shows the data for fully closed low-speed adjustments and 3 rotations on each high-speed adjustment. All graphs are included in **Figure 8**. It should be noted that a graph was not generated for the setting 0-4.3, because the miniature mill was unable to maintain the necessary velocity profile under high load. This is discussed further in the Issues and Future Improvements section of this paper. All settings were adjusted symmetrically to match the format of the published data accessible in [13].

The manufacturer-supplied curves published in [13] show the compression and rebound responses above and below the x-axis, respectively. After all measured data has been analyzed and plotted, it is possible to compare the measurements from the damper dynamometer to the manufacturer's published data. The graphs are first compared qualitatively, and it can be seen that there are certain observable similarities and differences between the plots. Like the manufacturer graphs, the measured force increases with higher settings, showing that the constructed dynamometer can clearly illustrate the difference between damper settings, and was able to measure the expected data trends. The measured data is visually different in the graphs of the 15-4.3, 25-4.3, and 0-0, in that there is a small velocity domain within the rebound response where the damping force decreases as the velocity increases. This is not seen in any of the manufacturer graphs and possibly suggests that the tests should be rerun. In addition, the quality of the different dynamometer systems can be seen in the graphed data. Because of noise in the measurement system of the constructed dynamometer, inconsistencies and discontinuities are common in the measured data, contrasted with the smoothly generated curves of the manufacturer data.

Quantitative analysis of the graphs allows for calculation and discussion of the error between the measured force output and that which is expected from the manufacturer data. For each run, the force output values are obtained from the measured

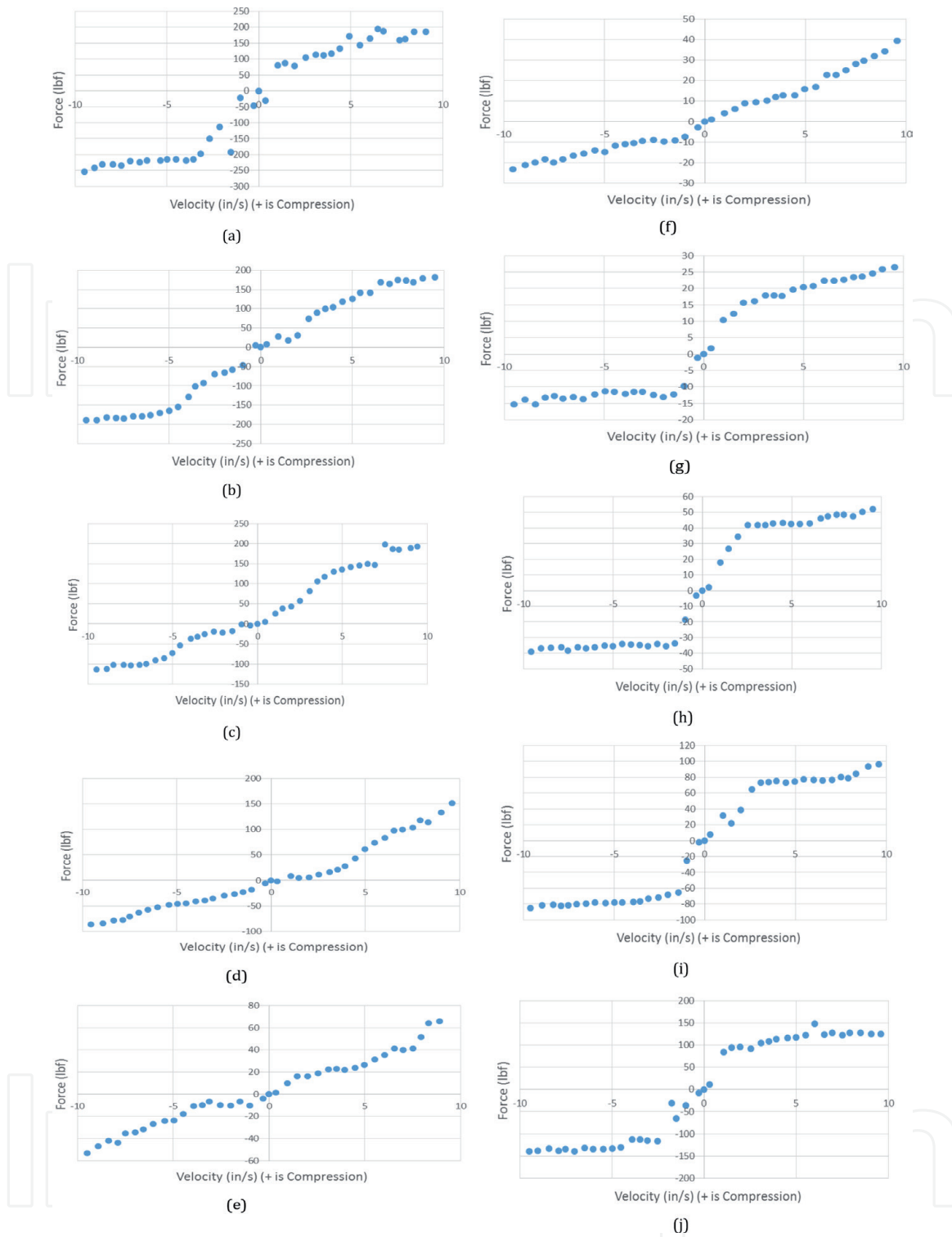


**Figure 8.** Force-Velocity Curves from Measured Data. (a) 2-4.3, (b) 4-4.3, (c) 6-4.3, (d) 10-4.3, (e) 15-4.3, (f) 25-4.3, (g) 0-0, (h) 0-1, (i) 0-2, (j) 0-3.

data at velocities of 5 in/s and 10 in/s, and these are compared to graphically obtained values at the same velocities from the published data [13]. These values and the associated error calculations are shown below in **Table 1**.

From **Table 1**, it can first be noted that the error values are overwhelmingly positive. This clear trend suggests that either a difference exists between the team's damper and a new one from the manufacturer, or that the dynamometer was improperly calibrated. Further investigation is necessary to determine which of these factors is the cause of this discrepancy.

Dataset	Measured @ 5 in/s (lbf)	Measured @ 10 in/s (lbf)	Manuf. @ 5 in/s (lbf)	Manuf. @ 10 in/s (lbf)	Error @ 5 in/s	Error @ 10 in/s
0-0 C	20	26	18	24	0.11	0.08
0-0 R	11	15	13	16	-0.15	-0.06
0-1 C	42	52	44	49	-0.05	0.06
0-1 R	35	40	31	37	0.13	0.08
0-2 C	75	100	75	92	0.00	0.09
0-2 R	80	85	58	63	0.38	0.35
0-3 C	115	125	107	125	0.07	0.00
0-3 R	135	145	80	103	0.69	0.41
2-4.3 C	145	190	115	150	0.26	0.27
2-4.3 R	210	250	94	130	1.23	0.92
4-4.3 C	125	180	96	140	0.30	0.29
4-4.3 R	165	190	73	115	1.26	0.65
6-4.3 C	140	190	70	130	1.00	0.46
6-4.3 R	75	110	57	105	0.32	0.05
10-4.3 C	60	150	38	100	0.58	0.50
10-4.3 R	50	90	30	75	0.67	0.20
15-4.3 C	25	60	25	65	0.00	-0.08
15-4.3 R	23	55	15	42	0.53	0.31
25-4.3 C	17	40	13	35	0.31	0.14
25-4.3 R	15	23	10	23	0.50	0.00

**Table 1.**  
*Measured and manufacturer data and calculated error.*

Cases averaged	Avg. error
Rebound	0.42
Compression	0.22
High-Speed sweep	0.14
Low-Speed sweep	0.44
Force <100 lbf	0.16
Force >100 lbf	0.51

**Table 2.**  
*Average error for comparison between case sets.*

Comparison between the average percent errors for certain segments of data gives insight into the areas where the constructed dynamometer is most accurate. These average values are listed in **Table 2** for easy comparison.

From this table, it should be noted that the measured data conforms more accurately to the published manufacturer data, in compression, than in rebound and shows much higher variation at higher loads and during low-speed sweep test

cases. Assuming the measured damper does have the performance characteristics of a new damper from the manufacturer, this variability between the datasets shows where the dynamometer is least accurate.

## 5. Issues and future improvements

The primary challenge associated with building this dynamometer at the lowest possible price point was integrating parts the team already owned rather than purchasing them, while at the same time creating a dynamometer that produces accurate measurements. Certain issues with the design could be solved with more work, and likely will be as the team continues to use the dynamometer, thus are discussed here.

Firstly, the measurement circuit should be improved to limit electronic noise in the measurements. As designed, all the circuitry between the sensors and the Genuino is constructed on a breadboard, which has the drawback of loose connections causing changes in the resistance of some circuit components during dynamometer operation. This was reduced where possible by using higher-resistance components, but a small movement in the connection of either of the nominal 350-ohm strain gauges can change their effective resistance by a significant percentage. This should be easily achievable by soldering resistors instead of using a breadboard. Limiting noise should provide better data for easier processing and would allow for more accurate determination of hysteresis present in the system, that may otherwise be overlooked.

The second primary issue with the dynamometer is that the miniature milling machine which provides the driving torque to the crank is unable to maintain a constant angular velocity under the load applied by the damper. In practice, this means the crank slows down when the connecting rod is at its most extreme angle to the damper and speeds up dramatically when the two are aligned. It is likely that this is the reason for the large percent error in higher-force tests. It is also hypothesized that this is one of the reasons for the large difference in error between rebound and compression cases. To address this issue, the team should consider obtaining permission to set up the damper dynamometer on a larger university milling machine. Not only would it likely be able to supply more torque and a more constant angular velocity, but it should also provide an overall stiffer framework for the dynamometer to operate within.

The present study can be converted into a course project for mechanical engineering students who take the vibrations and controls class to develop their hands-on experience and strengthen their understanding of the concepts of the dynamic behavior of vibration systems delivered in that class (**Table 3**) [14, 15].

Component	Price
Steel angles for frame	64.92
LM358 op-amp chips	6.99
Foil strain gauge sensors	13.99
Total	86.90

**Table 3.**  
*Price breakdown.*

## 6. Conclusion

To improve the performance of the FSAE car's suspension, the goal of this project was to design and build a low-cost dynamometer capable of producing a force-velocity curve for the car's dampers. Through the use of primarily pre-owned components, this dynamometer was constructed for less than 1/100 the price of market alternatives. Primary differences include the use of the team's milling machine to drive the dynamometer crank rather than a dedicated motor, and a cantilevered strain bar with strain gauges, custom wiring, and a Genuino to measure the force, rather than a dedicated load cell and computer system. While these changes offer great financial savings, this project has shown that they are not without their drawbacks. The graphs require calibration and data processing to produce and do not exactly replicate the manufacturer published values for the damper characteristics. This project, however, was still successful. It provided a completed and usable damper dynamometer, which through further testing and refinement will be able to accurately determine the characteristics of the team's dampers for a far lower cost than other methods.

## Conflict of interest

The authors declare no conflict of interest.

## Author details

Yucheng Liu<sup>1</sup> and Ge He<sup>2\*</sup>

<sup>1</sup> South Dakota State University, Brookings, USA

<sup>2</sup> University of Maryland, Baltimore, USA

\*Address all correspondence to: gh663@shu.edu.cn

## IntechOpen

© 2022 The Author(s). Licensee IntechOpen. This chapter is distributed under the terms of the Creative Commons Attribution License (<http://creativecommons.org/licenses/by/3.0>), which permits unrestricted use, distribution, and reproduction in any medium, provided the original work is properly cited. 

## References

- [1] Stanikzai MH et al. Seismic response control of base-isolated buildings using tuned mass damper. *Australian Journal of Structural Engineering*. 2020;**21**(1):310-321
- [2] Matin A, Elias S, Matsagar V. Distributed multiple tuned mass dampers for seismic response control in bridges. *Proceedings of the Institution of Civil Engineers-Structures and Buildings*. 2020;**173**(3):217-234
- [3] Elias S. Effect of SSI on vibration control of structures with tuned vibration absorbers. *Shock and Vibration*. 2019;**2019**:12. Article ID: 7463031. DOI: 10.1155/2019/7463031
- [4] Khanna A, Kaur N. Vibration of non-homogeneous plate subject to thermal gradient. *Journal of Low Frequency Noise, Vibration and Active Control*. 2014;**33**(1):13-26
- [5] Liu Y-C. Modeling abstractions of vehicle suspension systems supporting the rigid body analysis. *International Journal of Vehicle Structures & Systems*. 2010;**2**(3-4):117-126
- [6] Liu Y-C. Recent innovations in vehicle suspension systems. *Recent Patents on Mechanical Engineering*. 2008;**1**(3):206-210
- [7] Liu Y-C. Design of instructional tools to facilitate understanding of fluid viscous dampers in a vibration and controls class and course assessment. In: 2020 ASEE Virtual Annual Conference. Washington, D.C.: American Society for Engineering Education; June 22-26. 2020
- [8] Liu Y-C, Batte JA, Collins ZH, Bateman JN, Atkins J, Davis M, et al. Mechanical design, prototyping, and validation of a Martian robot mining system. *SAE International Journal of Passenger Cars—Mechanical Systems*. 2017;**10**(1):1289-1297
- [9] Liu Y-C, Meghat V, Machen B. Design and prototyping of a debris clean and collection system for a cylinder block assembly conveying line following an engineering systems design approach. *International Journal of Design Engineering*. 2018;**8**(1):1-18
- [10] Liu Y-C, Meghat V, Machen B. Design and prototyping of an *in situ* robot to clean a cylinder head conveying line following an engineering systems design approach. *International Journal of Design Engineering*. 2017;**7**(2):106-122
- [11] Liu Y, Whitaker S, Hayes C, Logsdon J, McAfee L, Parker R. Establishment of an experimental-computational framework for promoting Project-based learning for vibrations and controls education. *International Journal of Mechanical Engineering Education*. 2022;**50**(1):158-175. DOI:10.1177/0306419020950250
- [12] Liu Y-C. Implementation of MATLAB/Simulink into a vibration and control course for mechanical engineering students. In: ASEE SE Section Annual Conference; Auburn University, Auburn, AL, USA, Washington, D.C.: American Society for Engineering Education; March 8-10. 2020
- [13] Available from: <http://www.ohlinsusa.com/files/TTX25%20MkII%20Dyno%20lbs%20vs%20ips.pdf> [Accessed: August 31, 2020]
- [14] Liu Y-C, Baker F, He W-P, Lai W. Development, assessment and evaluation of laboratory experimentation for a mechanical vibrations and controls course. *International Journal of Mechanical Engineering Education*. 2019;**47**(4):315-337
- [15] Liu Y-C, Baker F. Development of vibration and control systems through

student projects. In: ASEE SE Section  
Annual Conference; North Carolina State  
University, Raleigh, NS, USA,  
Washington, D.C.: American Society for  
Engineering Education; March 10-12. 2019

IntechOpen

IntechOpen